*Journal of Chemistry and Technologies*, 2025, *33*(1), 249-261

**Journal of Chemistry and Technologies**

pISSN 2663-2934 (Print), ISSN 2663-2942 (Online).

*journal homepage*: http://chemistry.dnu.dp.ua
*editorial e-mail:* chem.dnu@gmail.com

**UDC 547.724**

# EFFECTIVE IMPROVEMENT OF HYDROGEN SULFIDE ADSORPTION FROM BIOGAS BY MEANS OF WATER TREATMENT SLUDGE AFTER ITS ZINC MODIFICATION

Vo Thi Thanh Thuy[1,2], Nguyen Thi Thuy[2,3], Le Si Qui[1,2], Lam Pham Thanh Hien[1,2], Ngo Thi Ngoc Lan Thao[1,2], Nguyen Thi Cam Tien[1,2], Dang Van Thanh[4], Trinh Thi Bich Huyen[1,2], Nguyen Nhat Huy[1,2*]

[1]*Faculty of Environment and Natural Resources, Ho Chi Minh City University of Technology (HCMUT), 268 Ly Thuong Kiet Street, District 10, Ho Chi Minh City, Vietnam*

[2]*Vietnam National University Ho Chi Minh City, Linh Trung Ward, Thu Duc City, Ho Chi Minh City, Vietnam*

[3]*School of Chemical and Environmental Engineering, International University, Quarter 6, Linh Trung Ward, Thu Duc City, Ho Chi Minh City, Vietnam*

[4]*Faculty of Basic Sciences, TNU-University of Medicine and Pharmacy, 284 Luong Ngoc Quyen St., Thai Nguyen City, Thai Nguyen Province, Vietnam*

*Received 17 July 2024; accepted 22 October 2024; available online 15 April 2025*

## Abstract

**In this study, waste sludge from different water treatment plants in Ho Chi Minh City, Vietnam, was used as adsorbents for $H_2S$ filtration in biogas. The results of the experimental process showed that the sludge calcined at 200 °C then modified with $Zn(NO_3)_2.6H_2O$ could reach an $H_2S$ adsorption capacity of 235.54 mg/g with operating conditions at 1775±169 ppm of $H_2S$ inlet concentration, 5 g of adsorbent, and 1 L/min of flow rate. Under the best conditions, the maximum adsorption capacity estimated by the Langmuir adsorption isotherm model can be up to 333.30 mg/g. Brunauer-Emmett-Teller method, X-ray diffraction, Fourier transform infrared spectroscopy, and scanning electron microscopy and energy-dispersive X-ray spectroscopy were the techniques used to determine material characteristics before and after adsorption. These results prove that sludge from wastewater treatment plants is a potential resource for the production of cheap but effective materials for environmental treatment.**

*Keywords:* biogas; $H_2S$ adsorption; utilizing solid waste; water treatment sludge.

# ЕФЕКТИВНЕ ПОКРАЩЕННЯ АДСОРБЦІЇ СІРКОВОДНЮ З БІОГАЗУ ЗА ДОПОМОГОЮ ОСАДУ ВОДОПІДГОТОВКИ ПІСЛЯ ЙОГО МОДИФІКАЦІЇ ЦИНКОМ

Во Тхі Тхань Туй[1,2], Нгуєн Тхі Туй[2,3], Ле Сі Куі[1,2], Лам Фам Тхань Хієн[1,2], Нго Тхі Нгок Лан Тхао[1,2], Нгуєн Тхі Кам Тієн[1,2], Данг Ван Тхань[4], Трінь Тхі Біч Хуєн[1,2], Нгуєн Нхат Хуй[*1,2]

[1]*Факультет екології та природних ресурсів, Хошимінський міський технологічний університет (HCMUT), вул. Лі Тхуонг Кьєт, 268, район 10, Хошимін, В'єтнам*

[2]*В'єтнамський національний університет Хошиміну, Лінь Трунг Вард, Ту Дук Сіті, Хошимін, В'єтнам*

[3]*Школа хімічної та екологічної інженерії, Міжнародний університет, квартал 6, Лінь Трунг Вард, Ту Дук Сіті, Хошимін, В'єтнам*

[4]*Факультет фундаментальних наук, Університет медицини та фармації ТНУ, вул. Луонг Нгок Куєн, 284, м. Тхай Нгуєн, провінція Тхай Нгуєн, В'єтнам*

## Анотація

**У цьому дослідженні відпрацьований мул з різних водоочисних станцій міста Хошимін, В'єтнам, використовувався як адсорбент для фільтрації $H_2S$ в біогазі. Результати експериментального процесу показали, що мул, прожарений при 200 °C, а потім модифікований $Zn(NO_3)_2{\cdot}6H_2O$, може досягти адсорбційної здатності H2S 235.54 мг/г за умов експлуатації при концентрації H2S на вході 1775±169 ppm, 5 г адсорбенту і швидкості потоку 1 л/хв. За найкращих умов максимальна адсорбційна ємність, розрахована за моделлю ізотерми адсорбції Ленгмюра, може становити до 333.30 мг/г. Для визначення характеристик матеріалу до і після адсорбції використовували метод Брунауера-Еммета-Теллера, рентгенівську дифракцію, інфрачервону спектроскопію з перетворенням Фур'є, а також растрову електронну мікроскопію та енергодисперсійну рентгенівську спектроскопію. Отримані результати доводять, що осад очисних споруд є потенційним ресурсом для виробництва дешевих, але ефективних матеріалів для очищення довкілля.**

*Ключові слова:* біогаз; адсорбція $H_2S$; утилізація твердих відходів; мул водоочищення.

**Corresponding author: e-mail: nnhuy@hcmut.edu.vn*

*doi: 10.15421/jchemtech.v33i1.308661*

*Journal of Chemistry and Technologies*, 2025, *33*(1), 249-261

## Introduction

Biogas is a source of biological energy widely used as an alternative to natural gas in life and industry. The wastes from agricultural activities provide raw materials for the biogas production process, and the generated gas can be used directly in households. On an industrial scale, biogas from anaerobic digestion can be used as a fuel for electricity generators to help reduce production costs and greenhouse gas emissions. However, the heat generated when burning 1 $m^3$ of raw biogas is about 21.5 MJ, which is 1.67 times lower than the heat of 1 $m^3$ of pure $CH_4$. This is because raw biogas contains impurities other than $CH_4$ such as $CO_2$, $H_2$, $O_2$, $H_2S$, and $NH_3$. In which, $H_2S$ is the main cause of the odor (bad smell of $H_2S$) and air pollution ($SO_2$ from the combustion process). The concentration of $H_2S$ in biogas depends on many factors (e.g., anaerobic technology, raw organic material, and capacity of digester), in the range of 50 to 5000 ppm or up to 20000 ppm [1]. In addition, the presence of $H_2S$ also causes pipeline corrosion, thus reducing the lifetime of equipment and structures. Moreover, $H_2S$ is also a toxic gas and has an unpleasant odor that directly affects health and can lead to death when exposed to high concentrations.

On the other hand, the sludge generated from the supply water treatment process (water treatment sludge, WTS) with large discharge into the environment is a big challenge for management and treatment. This discharge is usually higher on days when the treatment plant discharges sludge from the settling tank. With a diverse composition of metal elements (i.e. Fe, Al, Cu, Zn,…)[2-5] , WTS can be utilized for many different purposes, especially as $H_2S$ adsorbent [3, 4] or phosphorus adsorption [5]. Iron is an element that often occurs in highly efficient $H_2S$ adsorbents since $Fe^{2+}$ can react directly with $H_2S$ to produce FeS (black) or can act as a catalyst to oxidize sulfide ($S^{2-}$) to elemental sulfur ($S^0$) [6]. The utilization of sewage sludge and WTS for $H_2S$ adsorption has been reported in many studies. The alum sludge modified at different temperatures gave different $H_2S$ treatment capacities. In which, the best $H_2S$ filtration capacity belongs to the sludge calcined at 300 °C [3]. The addition of iron significantly improved the treatment capacity of WTS as demonstrated in the study of Polruang, Banjerdkij [4] with an adsorption capacity of 105.22 mg$H_2S$/g. Ren, Lyczko [7] suggested that the metal mineral composition, microporous structure, and alkaline pH in the waterworks residue promote $H_2S$ adsorption due to the formation of metal sulfate species. Iron-based catalysts calcined at 500 °C derived from sludge were developed for efficient $H_2S$ oxidation [8]. Optimization with 2 M NaOH further enhanced catalytic activity, attributed to improved surface properties, higher $Fe^{3+}$ content, and increased oxygen vacancies.

In this study, WTS from different supply water plants were collected, modified, and applied for $H_2S$ adsorption. The influences of $H_2S$ concentration and the amount of adsorbent were investigated. In addition, the possibility of material regeneration by heating was also studied. A comparative experiment with commercial adsorbents was also conducted to form the basis for the material development in further studies.

## Materials and Methods

*Materials*

The chemicals used in the experiments are sourced from China and are highly purified. The WTS used in this study was collected from water supply plants in Ho Chi Minh City, Vietnam (i.e., Tan Hiep, Thu Duc, Tan Phu, and BOO Thu Duc). The raw sludge was dried at 105 °C, ground, and sieved to the desired size (0.105−2 mm) as shown in Fig. 1. After that, the WTS was modified with HCl, $H_3PO_4$, $NaHCO_3$, $Zn(NO_3)_2.6H_2O$, and $Mg(NO_3)_2.6H_2O$. The modification process was based on previous publications [9-11] with some changes to adapt it to the actual conditions.Chemicals and abbreviated names of the modified materials are summarized in Table 1, where WTS can be replaced by TH, TD, TP, and BOO representing sludge from the water treatment plants of Tan Hiep, Thu Duc, Tan Phu, and BOO Thu Duc, respectively. The acid-modified WTS was prepared by mixing 1 g of WTS with 1 mL of acid solution (commercial concentration), which was then stirred for 30 min, filtered and washed with distilled water to pH 7, and finally dried at 105 °C for 24 h. The impregnation of WTS with $NaHCO_3$ was conducted by mixing 3 g WTS with 33 mL of 1 M $NaHCO_3$ solution, stirring and aeration for 30 min (2 L/min), then filtering and washing with distilled water to pH 7, and drying at 105 °C for 24 h. Regarding the modification of WTS by metal ions, 10 g WTS was added to 200 mL of 0.25 M salt solution, which was then added with 800 mL of distilled water. Next, the pH was adjusted to 11 by 30 % $NH_4OH$ solution and the solution was ultrasonically treated for 1 h. Subsequently, the material was filtered and washed with distilled water to pH 7 and dried at 105 °C for 12 h. The modified WTS with

*Journal of Chemistry and Technologies*, 2025, *33*(1), 249-261

$Mg(NO_3)_2.6H_2O$ and $Zn(NO_3)_2.6H_2O$ were denoted as Mg/WTS and Zn/WTS, respectively. In addition, Zn/TP materials were also selected to investigate the effect of thermal treatment (e.g., calcined at 200 °C for 6 h). The order of thermal treatment in material modification is also of interest as we compare two materials of 200 °C-calcined TP sludge + modified with $Zn(NO_3)_2.6H_2O$ (200-Zn/TP) and $Zn(NO_3)_2.6H_2O$-modified TP sludge + calcined at 200 °C (Zn/TP-200).

Raw sludge | Dried sludge, 105 °C | Ground sludge

**Fig. 1. WTS before modification**

*Table 1*

**Abbreviation of modified adsorbents**

| Adsorbent* | Ratio adsorbent:chemical | Chemical | Reference |
|---|---|---|---|
| WTS-HCl | 1 g : 1 mL (commercial solution) | HCl | [9] |
| WTS-$H_3PO_4$ | | $H_3PO_4$ | |
| WTS-$NaHCO_3$ | 3 g : 33 mL (solution, 1 M) | $NaHCO_3$ | [10] |
| Zn/WTS | 10 g : 200 mL (solution, 0.25 M) | $Zn(NO_3)_2.6H_2O$ | [11] |
| Mg/WTS | | $Mg(NO_3)_2.6H_2O$ | |

*WTS can be replaced by TH, TD, TP, and BOO representing sludge from Tan Hiep, Thu Duc, Tan Phu, and BOO Thu Duc water treatment plants, respectively.

The material properties such as surface area, crystalline structure, surface functional groups, morphology, and elemental composition were determined by the Brunauer-Emmett-Teller method (BET, Nova 4000E, Quantachrome, USA), X-ray diffraction (XRD, D2 Phaser, Bruker), Fourier transform infrared spectroscopy (FTIR, Tensor 27, Bruker), and scanning electron microscopy and energy-dispersive X-ray spectroscopy (SEM-EDX, JSM-IT200, JEOL), respectively.

*$H_2S$ adsorption experiment*

The $H_2S$ adsorption experiment was set up as shown in Fig. 2. The concentrated $H_2S$ stream was formed by the reaction between $Na_2S.9H_2O$ and 10 % $H_2SO_4$ solution (Flow 1). A stabilizer was arranged to make it easier to control the gas flow concentration. Flow 2 is the air that is pumped to the air tee and mixed with Flow 1. The gas flow rate was controlled by the flowmeter so that the total treatment flow was kept constant during the tests. The adsorbent was placed in a 26 mm diameter mica tube and the gas flows through the adsorbent layer in the top-down direction. Gaseous $H_2S$ was analyzed by absorption spectroscopy at 670 nm according to Vietnam standard (10 TCN 676-2006 – Ministry of Agriculture and Rural Development).

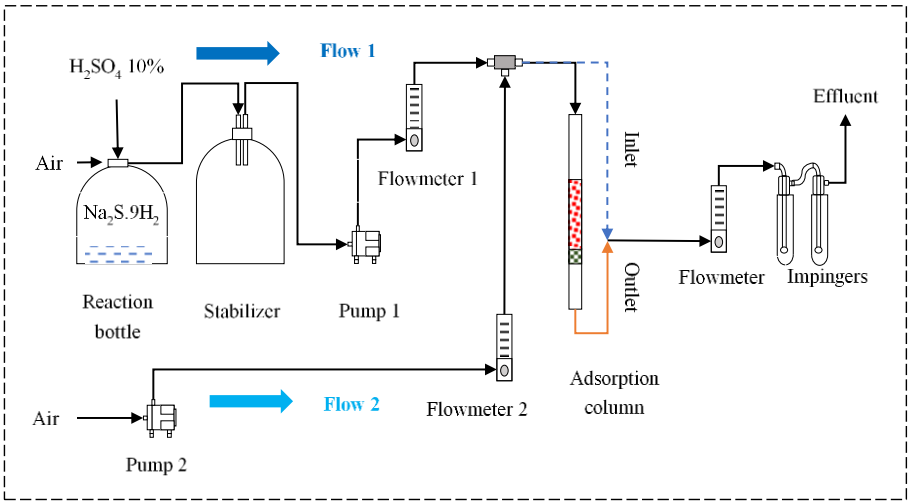


**Fig. 2. $H_2S$ adsorption experiment system**

*Journal of Chemistry and Technologies*, 2025, *33*(1), 249-261

The experiments were conducted as shown in Fig. 3, and the $H_2S$ removal efficiency was recorded when changing the adsorbent, adsorbent amount (2.5, 5, 7.5, and 10 g), and initial concentration (1000, 1500, 2000, 2500, and 3000 ppm) with 1 L/min of flowrate. The $H_2S$ removal efficiency (RE, %) was calculated by Equation 1, where $C_{in}$ and $C_{out}$ are the $H_2S$ inlet and outlet concentrations, respectively.

$$RE = \left(1 - \frac{C_{out}}{C_{in}}\right) \times 100\ \% \quad (1)$$

Langmuir and Freundlich isotherm models were applied to determine the adsorption parameters for the $H_2S$ adsorption process (Equations 2 and 3). Where $C = C_{in}$ is the $H_2S$ initial concentration (mg/m$^3$). a and $a_{max}$ are the capacity and its maximum value (mg/g), and $K_L$, $K_F$, and n are the adsorption constants (0 < n <1).

$$\frac{C}{a} = \frac{1}{a_{max}}\left(\frac{1}{K_L} + C\right) \quad (2)$$

$$lna = lnK_F + n \times lnC \quad (3)$$

The reusability of the material was also investigated using a desorption experiment. The material after the first adsorption was desorbed by heating for 2 h at different temperatures (200, 300, and 400 °C) and by blowing air over the material layer for 4 h at a gas flow rate of 2 L/min.

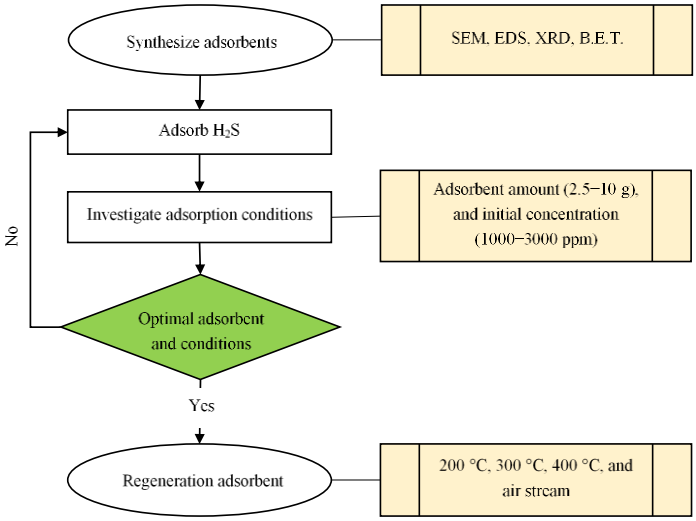


**Fig. 3. Research experiment diagram**

## Results and Discussion

### *Effect of adsorbent*

The adsorbent is a key factor in the adsorption process and the $H_2S$ removal efficiency of different adsorbents was first investigated. As shown in Fig. 4, the adsorption capacity depended on the raw sludge origin and the modification method, in which, the acid modification proved ineffective when the capacity fluctuated in the range of 3.9–10.6 mg/g with WTS-HCl and 9.3–19.4 mg/g with WTS-$H_3PO_4$. Actually, the use of acid can dissolve the mineral components in the raw sludges, thus helping to strengthen the porous structure of the material and increasing the surface area. However, the acid solution can strongly reduce the adsorption efficiency of the adsorbent by reacting with metal elements to lose the metal adsorption centers and reacting with available alkaline elements to reduce the efficiency of acid gas such as $H_2S$.

The WTS-$NaHCO_3$ had a higher $H_2S$ adsorption capacity than WTS-HCl and WTS-$H_3PO_4$ for the sludge from the Tan Phu Plant and Thu Duc Plant. Specifically, for the sludge from Tan Phu Plant, the adsorption capacity of TP-$NaHCO_3$, TP-HCl, and TP-$H_3PO_4$ were 61.8, 10.6, and 17.7 mg/g, respectively. For the sludge from Thu Duc Plant, the values were 47.8, 6.2, and 9.3 mg/g, respectively. Thus, for these two plants, modification with acid and bicarbonate resulted in adsorption capacities in the order of WTS-$NaHCO_3$ > WTS-$H_3PO_4$ > WTS-HCl. Meanwhile, for sludge samples from BOO Plant and Tan Hiep Plant, modification with $H_3PO_4$ yielded better results than $NaHCO_3$, but the difference was not significant. The adsorption capacities of BOO/TH-$NaHCO_3$, BOO/TH-HCl, and BOO/TH-$H_3PO_4$ were 3.5/4.3, 19.4/9.0, and 3.9/3.5 mg/g, with the order of WTS-$H_3PO_4$ > WTS-$NaHCO_3$ > WTS-HCl. This difference may be due to the different elemental compositions (high density) of these sludge types. Tan Phu Plant treats iron-contaminated groundwater while Thu Duc Plant uses iron salt as a coagulant for surface water treatment. Therefore, the iron content available in the sludge from these two plants is quite high,

*Journal of Chemistry and Technologies*, 2025, *33*(1), 249-261

which can react with $NaHCO_3$ to create the α-FeOOH phase that promotes the $H_2S$ adsorption [10].

For sludges impregnated with $Mg^{2+}$ (Mg/WTS) and $Zn^{2+}$ (Zn/WTS), the adsorption efficiency was significantly improved in all sludge samples as compared with materials modified by other methods. This may be because the layered double hydroxide (LDH) structure, which is similar to the mineral hydrotalcite, forms with the co-occurrence of added bivalent metal elements ($Mg^{2+}$ and $Zn^{2+}$) and available trivalent metal in the sludge ($Fe^{3+}$) [12; 13]. With their basic surface and large specific surface area, LDH-structured materials are an excellent choice for acid gas adsorption such as $H_2S$ [14]. Mg is reported to be in the element group that combines more with sulfur in anionic clays, along with Al, Ni, Fe, and Cu [14]; therefore, this enhanced the $H_2S$ adsorption capacity of Mg/WTS. On the other hand, ZnO belongs to the oxide group with good desulfurization ability at high temperatures [14], room temperature [15], and moist condition [16]. According to a report on the physicochemical composition of the WTS from Tan Hiep, Tan Phu, and Thu Duc Plants [2], the iron element content (%w/w) in the sludge sample from the Tan Phu Plant was the highest, followed by Thu Duc sludge, and the lowest is Tan Hiep sludge. This explained the outstanding $H_2S$ adsorption ($2Fe^{n+} + nH_2S \rightarrow Fe_2S_x$ (black) + $2nH^+$).

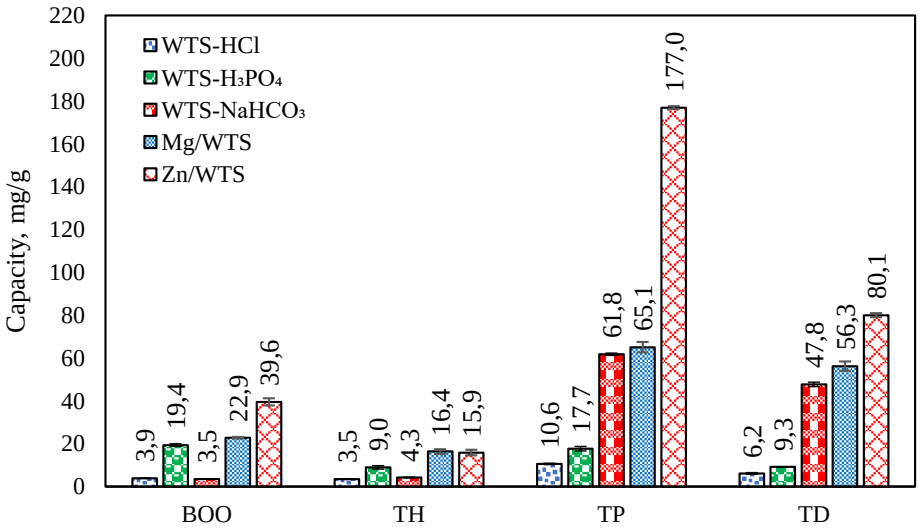


**Fig. 4. The $H_2S$ capacity of different adsorbents (operating conditions: 1775 ± 169 ppm of $H_2S$, 5 g of adsorbent, and flow rate of 1 L/min)**

The influence of thermal modification as well as the order of the thermal modification step in the material modification process was also investigated with three adsorbent materials of Zn/TP, 200-Zn/TP, and Zn/TP-200 (Fig. 5). These results showed that the thermal treatment step clearly affects the adsorption process. Specifically, the adsorption capacity increased in the order of Zn/TP < Zn/TP-200 < 200-Zn/TP with 166.30 < 186.70 < 235.54 mg/g, respectively. When the material is heated at a high temperature (200 °C), volatile components are removed and the pore volume is increased, thereby improving the adsorption ability of the material. The thermal treatment step was performed before the $Zn^{2+}$-impregnating process to help solidify the sludge structure and convert dissolved cation forms into more stable oxides. This avoids the metals being washed away during the impregnation process and increases the number of adsorption centers on the material surface for $H_2S$ adsorption. This would be the main reason for the strong enhancement of the $H_2S$ removal efficiency and adsorption capacity of 200-Zn/TP materials.

In order to better understand the process of the $H_2S$ adsorption by materials from the water treatment plant, the raw sludge from Tan Phu Water Treatment Plant, 200-Zn/TP before and after adsorption (200-Zn/$TP_{ba}$ and 200-Zn/$TP_{aa}$) were selected to analyze some material characteristics by SEM, EDX, XRD, FTIR, and BET. The SEM images in Fig. 6 show that the surface of Tan Phu-raw sludge and 200-Zn/$TP_{ba}$ is relatively different. Tan Phu-raw sludge has a smooth surface and slight roughness, which may be due to the presence of sand particles in the WTS [17]. They are usually larger than the rest of the ingredients (Fig. 6a). In addition, the observed rough surfaces can be attributed to the presence of precipitated heavy metals, such as calcium and iron present in the sludge [18; 19].

*Journal of Chemistry and Technologies*, 2025, *33*(1), 249-261

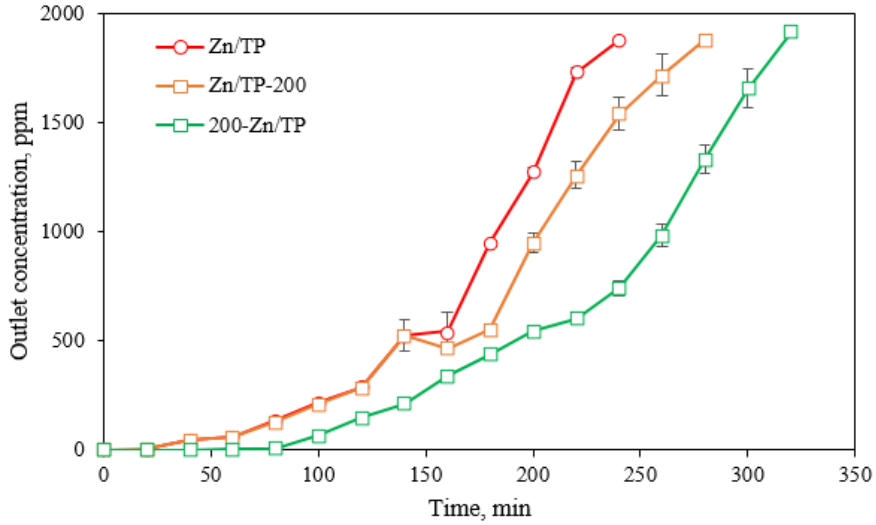


**Fig. 5. Breakthrough curve of $H_2S$ adsorption with Zn/TP, Zn/TP-200, and 200-Zn/TP (operating conditions: 1775 ± 169 ppm of $H_2S$, 5 g of adsorbent, and flow rate of 1 L/min)**

These particles are smaller in size as compared to other components in the slurry and have been observed to form clumps and occupy part of the sand surface. Fig. 6b shows that the 200-TP-$Zn_{ba}$ material has a more porous structure than the coarse sludge, and the smooth or slightly rough surfaces were reduced. After being impregnated with $Zn^{2+}$ in an $NH_4OH$ environment, more precipitates were formed on the surface of the material than in the raw sludge.

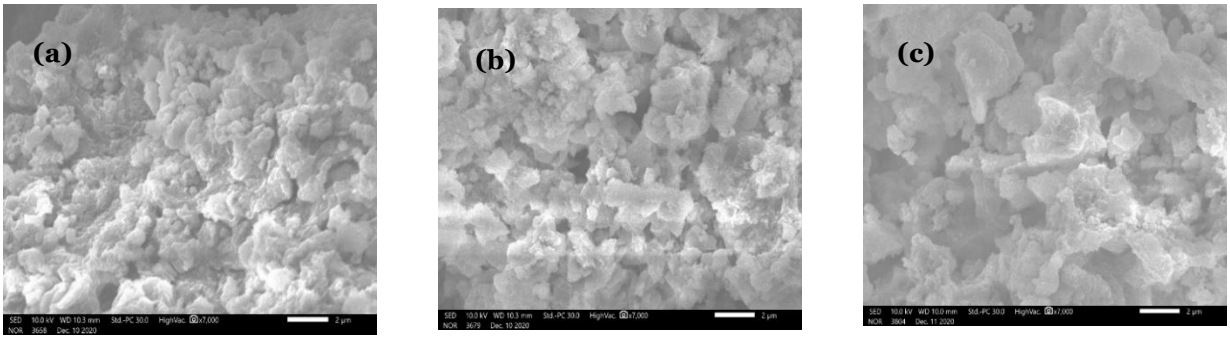


**Fig. 6. SEM images of (a) Tan Phu-raw sludge, (b) 200-Zn/TP before adsorption (200-Zn/$TP_{ba}$), and (c) 200-Zn/TP after adsorption (200-Zn/$TP_{aa}$)**

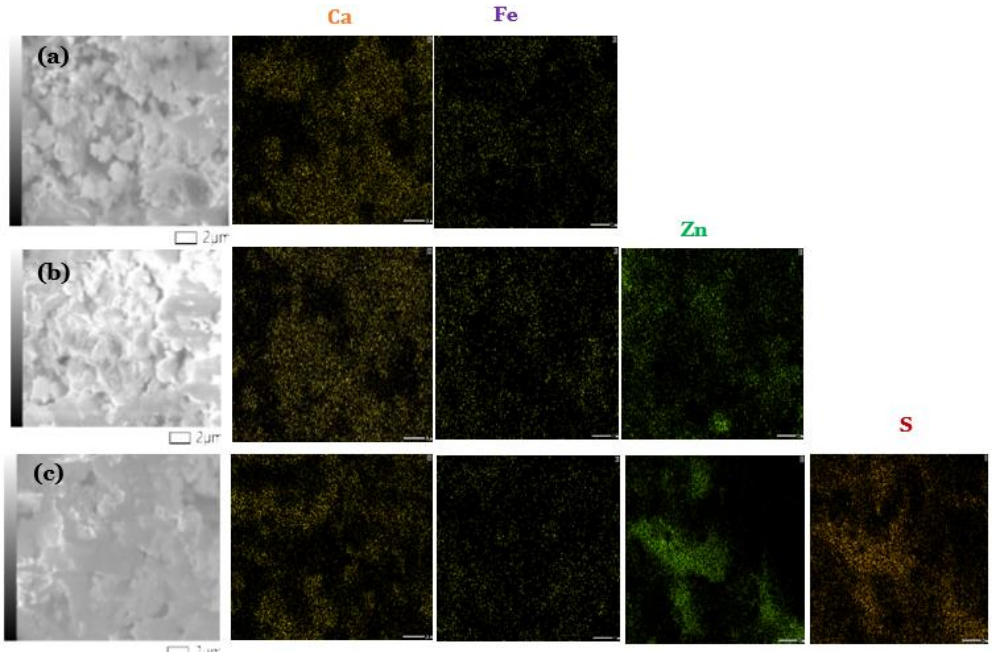


**Fig. 7. SEM-EDX Mapping of (a) Tan Phu-raw sludge, (b) 200-Zn/TP before adsorption (200-Zn/$TP_{ba}$), and (c) 200-Zn/TP after adsorption (200-Zn/$TP_{aa}$)**

*Journal of Chemistry and Technologies*, 2025, *33*(1), 249-261

The SEM-EDX mapping result in Fig. 7b shows the presence of Zn element on the surface of 200-TP-$Zn_{ba}$ material (~5.60 % w/w). This confirmed that the 200-TP-Zn material was successfully prepared. After the adsorption, the $H_2S$ gas molecules adhere to the surface of the adsorbent and insert into the pores, thus making the surface of the 200-TP-$Zn_{aa}$ less rough (Fig. 6c). Sulfur was also found in the 200-TP-$Zn_{aa}$ sample (Fig. 7c) with a ratio of 9.64 % w/w, indicating that $H_2S$ was really retained after passing the adsorbent column. The active Ca element in Tan Phu sludge (Fig. 7) originates from the use of $Ca(OH)_2$ at this plant as an alkaline element that is beneficial for the adsorption of acidic gases such as $H_2S$. However, Fig. 7c shows that the positions of S are almost similar to those of Fe and Zn, proving that Fe and Zn are the major active centers of $H_2S$ adsorption in this study.

The crystalline characteristics are shown by XRD results in Fig. 8. Tan Phu-raw sludge and 200-Zn/$TP_{ba}$ samples have similar peaks at 2θ of 22.10°, 26.67°, 29.33°, 36.10°, 35.56°, 43.17°, 47.40°, 48.40°, and 57.56°, which are characteristics for $CaCO_3$ (card No. 01-089-1304). After the adsorption process, the XRD spectrum of the Zn-modified sludge calcined at 200 °C appeared more peaks at 11.5°, 14.8°, 25.5°, and 37.4° for FeS (card No. 00-037-0047), 24.6° and 28.7° for $Fe_3S_4$ (card No. 01-089-1998), 21.9°, 27.7°, 31.5°, and 36.2° for ZnS (card No. 00-036-1450), and 23.2° and 26.6° for $CaSO_4$ (card No. 00-055-0954). Thus, both SEM-EDX mapping and XRD pattern indicate that Fe and Zn are present in 200-Zn/$TP_{ba}$ with an amorphous form. From the above results, chemical adsorption is predicted to be the main adsorption mechanism with the appearance of FeS, $Fe_3S_4$, ZnS, and $CaSO_4$ components in the material after $H_2S$ adsorption.

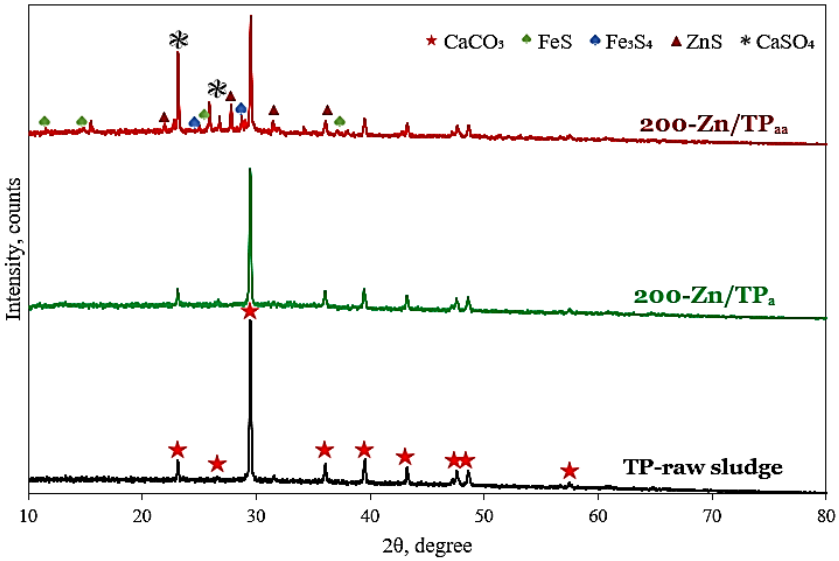


**Fig. 8. XRD patterns of Tan Phu-raw sludge, 200-Zn/TP before adsorption (200-Zn/$TP_{ba}$), and 200-Zn/TP after adsorption (200-Zn/$TP_{aa}$)**

The FTIR results of the three samples in Fig. 9 show that the spectrum of the raw sludge has vibration peaks at 3442, 2512, 1427, 1015, 875, and 712 $cm^{-1}$. The band at 3442 $cm^{-1}$ is thought to be a prolonged vibration of the hydroxyl groups [20] while the weak bands at 2512 and 1623 $cm^{-1}$ exhibit O–H bending vibrations of the adsorbed water molecules [21]. The weak peak at 1795 $cm^{-1}$ corresponds to the C=O bonds from the carbonate group [22]. The wide and deep band at 1427 $cm^{-1}$ may correspond to the iron oxides present in the sludge [23] or the bond of the C=O group from the carbonate group [22]. The medium and narrow band at 875 and 712 $cm^{-1}$ corresponds to Ca–O bonds [22] or calcium carbonate [24]. The weak band at 1020 $cm^{-1}$ may represent a hydroxyl group bound to Fe, Mg, or Si [23]. The FTIR of the Zn-modified sludge calcined at 200 °C has a peak at 2361 $cm^{-1}$ and the narrow band at 1020 $cm^{-1}$ was replaced by a wide band at 1031 $cm^{-1}$. This may be due to the association of the hydroxyl group with Zn and Fe during the preparation of 200-Zn/$TP_{ba}$ material. After adsorption, the peaks at position 2361 and 1031 $cm^{-1}$ were completely lost, indicating that the hydroxyl groups associated with Zn and Fe participated in the $H_2S$ reaction to form ZnS and FeS, which is consistent with the XRD results in Fig. 8. In addition, the peaks with weak intensity at 1150, 1005, 659, and 601 $cm^{-1}$ correspond to $SO_4^{2-}$ group bonding of metal oxides present in the material, mainly Ca [25].

*Journal of Chemistry and Technologies*, 2025, *33*(1), 249-261

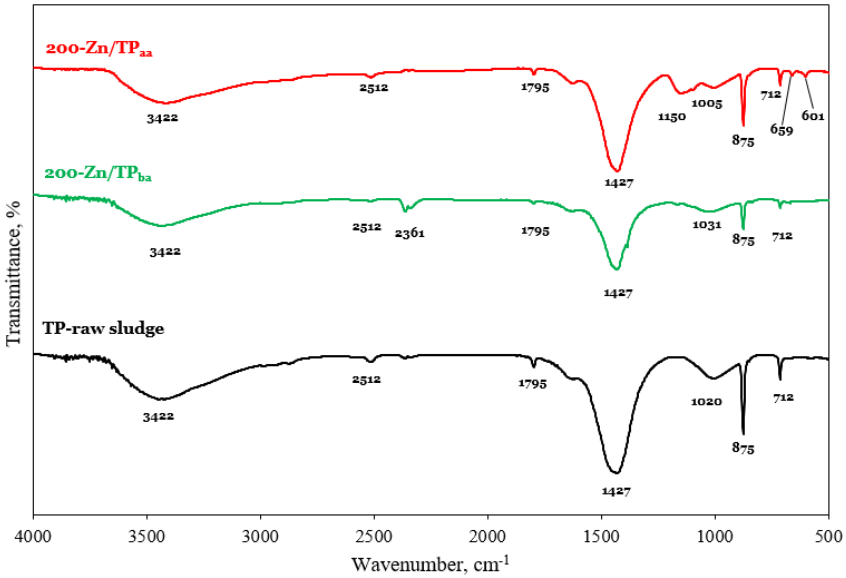


**Fig. 9. FTIR spectra of Tan Phu-raw sludge, 200-Zn/TP before adsorption (200-Zn/TP$_{ba}$), and 200-Zn/TP after adsorption (200-Zn/TP$_{aa}$)**

$N_2$ adsorption and desorption were carried out at −196 °C with 200-Zn/TP, the adsorption and desorption curves in Fig. 10 show that the material has a type IV adsorption isotherm. The amount of adsorption is low in the region of relatively low pressure ($P/P_o < 0.01$) while the adsorption and desorption isotherms have a steep slope in the region of high relative pressure ($P/P_o \sim 0.9–1.0$). This could be explained by the fact that the pores in the material are mainly mesopores [26; 27] similar to the pore size distribution. From the appearance of the type A hysteresis loop, it can be inferred that the 200-Zn/TP has some tubular pores. The BET surface of the 200-TP/Zn sludge is 89.51 $m^2/g$, much lower than that of other $H_2S$ adsorbents such as OMSs (MCM-41, 1141 $m^2/g$ [28]), activated carbon (BAX, 1000 $m^2/g$ [29]). Also, the pore size distribution in Fig. 10 shows that the material structure contains pores with sizes distributed from 3 to 100 nm, with a total pore volume of 0.2044 $cm^3/g$. However, most of pores are the mesopores with diameters mainly from 3.0 to 14.6 nm which coincides with the adsorption and desorption isotherms.

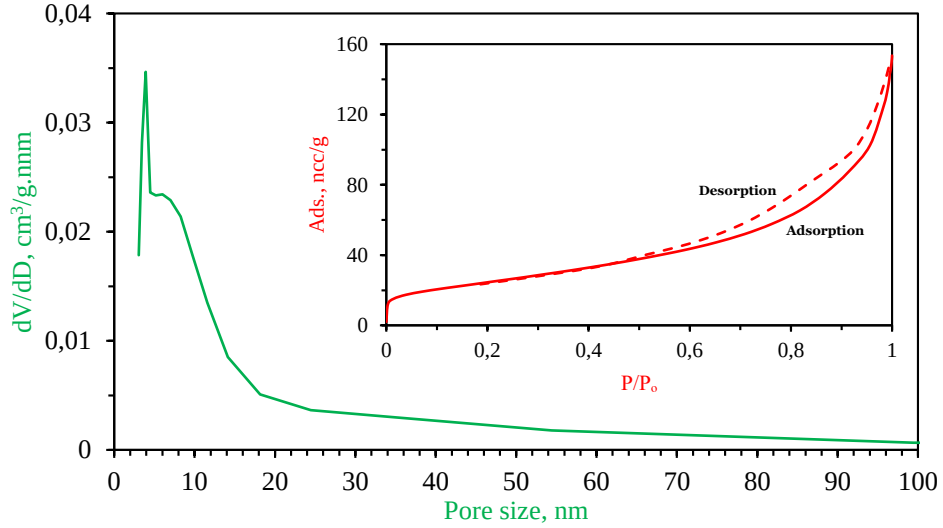


**Fig. 10. The adsorption and desorption isotherms and pore size distribution of 200-Zn/TP**

*Effect of empty bed contact time on efficiency*

Empty bed contact time (EBCT) is an important parameter characterizing the relationship between the volume of the adsorbent layer and gas flow rate. In this study, the effect of EBCT on the adsorption process was investigated with the change of adsorbent amount (2.5–10 g) when the treatment gas flow was fixed at 1 L/min and the initial $H_2S$ concentration was controlled at ~ 2410 ±169 ppm.

The breakthrough curves in Fig. 11 show that by increasing EBCT from 0.32 s to 1.32 s, the effective adsorption time (denoted as $t_b$, determined at the time when $C_{out} \sim 0$) increased

*Journal of Chemistry and Technologies*, 2025, *33*(1), 249-261

from 20 min to 460 min. This is completely consistent with the theory of adsorption in the contact time between the gas phase and the solid phase. As EBCT is enhanced, the mass transfer process is better and more $H_2S$ is retained in the material layer. This helps the airflow to be thoroughly treated for a longer time. Although increasing EBCT is beneficial for the adsorption process, this value will be limited in practice by the device pressure loss. In addition, to ensure the uniformly distributed gas flow, the uniformity of the adsorbent along with the size parameter of the material layer are also important factors in determining which EBCT value is appreciated. In this experiment, only the uniformity of the adsorbent was controlled (0.105–2 mm) while the remaining factors were assumed to have a negligible influence on the lab-scale system. The adsorption capacity of the materials with different EBCTs was also calculated. Accordingly, when using 2.5 g of 200-Zn/TP sludge, the adsorption capacity reached 199.9 mg$H_2S$/g and then this value increased to 1.45 times when using 10 g of adsorbent, reaching 289.1 mg$H_2S$/g, which is consistent with those reported in the literature [30] and our previous study [19].

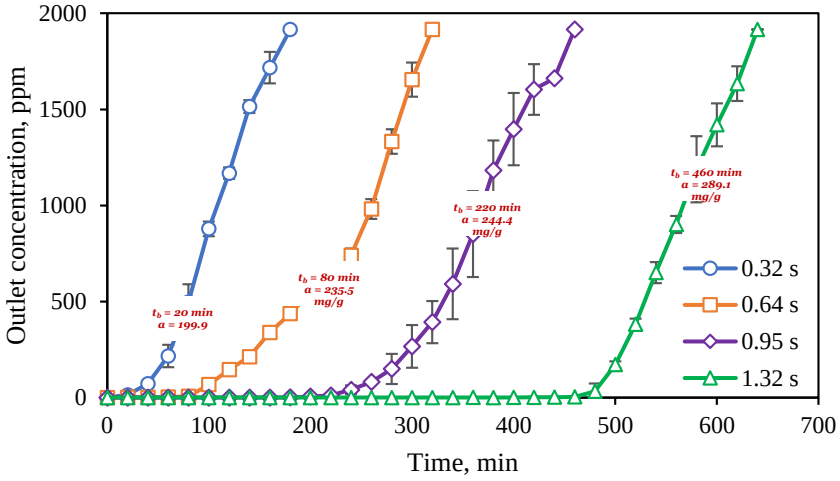


**Fig. 11. Breakthrough curve of $H_2S$ adsorption at different EBCT, $t_b$ - the effective adsorption time and a – the $H_2S$ adsorption capacity (operating conditions: 1733 ± 169 ppm of $H_2S$, 2.5–10 g of 200-Zn/TP, and 1 L/min of flow rate)**

*Effect of $H_2S$ initial concentration*

$H_2S$ adsorption tests were conducted at different initial concentrations in the range of 1000–3000 ppm, with 10 g of 200-Zn/TP sludge and a flow rate of 1 L/min. The $H_2S$ adsorption capacity in Fig. 12 shows that when the initial concentration increased from 1000 to 2500 ppm, the capacity also increased from 261.4 to 309.9 mg$H_2S$/g. However, if the $H_2S$ concentration continued to increase, the obtained capacity tended to decrease. For the mass transfer, when the contaminant concentration increases, the kinetics of the process is also improved, thereby increasing the adsorption efficiency. In addition, the tendency of multilayer adsorption can also be a reason for more efficient treatment. However, if the concentration of pollutants is too high, the adsorbent surface can quickly become saturated, and $H_2S$ cannot penetrate deeply into the pore system of the material, thus reducing the adsorption efficiency as well as the adsorption capacity. This result was similar to the study of Choo, Lau [31] when $H_2S$ was adsorbed by $K_2CO_3$-impregnated activated carbon.

According to the experiment at different $H_2S$ initial concentrations, Langmuir and Freundlich isotherms were applied to calculate characteristic parameters for the $H_2S$ adsorption process (Fig. 13). The results show that the $H_2S$ adsorption with 200-Zn/TP sludge in the range of 1000–3000 ppm $H_2S$ (~ 1390–4170 mg$H_2S$/m$^3$) described by Langmuir isotherm ($R^2$ = 0.9926) was more suitable than Freundlich isotherm ($R^2$ = 0.8583). This result is consistent with some of our previous studies on $H_2S$ adsorption by red mud [32] and alum sludge of water treatment plants [33]. At the same time, a study using oil-sludge-based adsorbents for $H_2S$ removal in oilfield gases also showed that the Langmuir isotherm fits better than the Freundlich isotherm [34]. The coefficient of conformity assessment of the Langmuir isotherm ($R_L$) was calculated to check the experiment results following Equation 4, where $K_L$ is the Langmuir constant in Equation 2 and $C_{in}$ is the $H_2S$ initial concentration (mg/m$^3$). All $R_L$ values in the investigated concentration were in the range of 0–1, indicating that the $H_2S$ adsorption with 200-Zn/TP described by Langmuir isotherm is completely consistent [35].

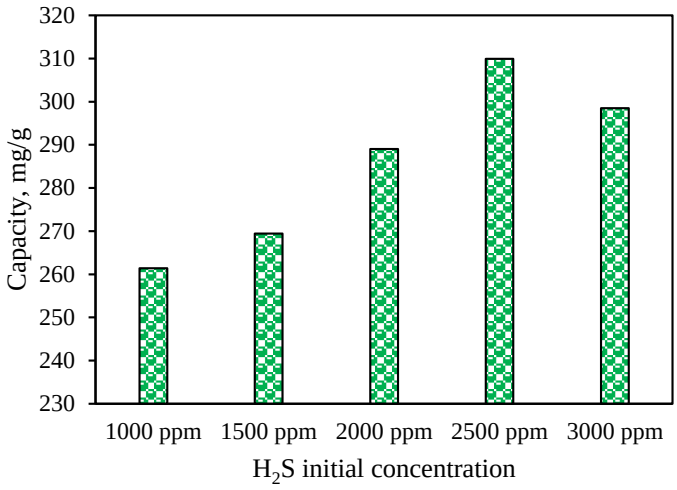


**Fig. 12. Effect of initial concentration on adsorption capacity (operating conditions: 1000−3000 ppm of $H_2S$, 10 g of 200-Zn/TP, and 1 L/min of flow rate)**

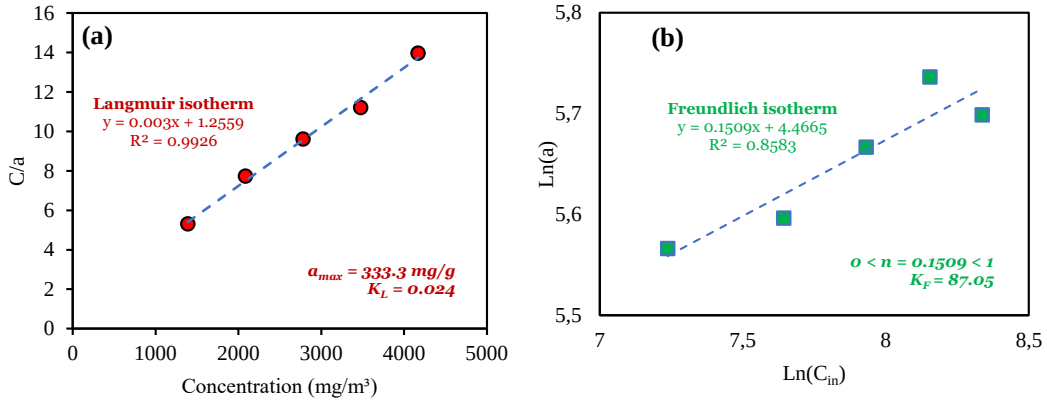


**Fig. 13. Langmuir isotherm (a) and Freundlich isotherm (b) of $H_2S$ adsorption with 200-Zn/TP**

Since this experimental process is more consistent with Langmuir isotherm, it can be predicted that monolayer adsorption is more dominant, the adsorption centers do not interact with each other, and the tendency for competitive adsorption is less. Compared with other studies (Table 2), the maximum adsorption capacity of 200-Zn/TP is somewhat superior. To be able to draw more conclusions, it is necessary to compare the adsorption capacity of adsorbents under the same conditions. However, this result is also remarkable in the effort to utilize water treatment sludge as $H_2S$ adsorbent.

$$R_L = \frac{1}{1 + K_L \times C_{in}} \quad (4)$$

*Table 2*

**$H_2S$ adsorption capacity of some materials**

| Adsorbents | Conditions | Capacity, mg/g | Langmuir/Freundlich | References |
|---|---|---|---|---|
| Cu/PAC 450 | T = 20 °C<br>[$H_2S$] = 100−500 ppm<br>Q = 2 mL/min | 95.66 | Langmuir<br>($R^2$ = 0.9627) | [36] |
| BL-450-6 | T = 293 K<br>[$H_2S$] = 80−800 ppm<br>Q = 1 L/min | 25.00 | Langmuir<br>($R^2$ > 099) | [37] |
| Si-CHA | T = 298 K<br>p = 0−190 kPa<br>m = 0.73 g | 194.48 | Langmuir<br>($R^2$ > 0.999) | [38] |
| MSA | T = 303 K<br>p = 0−1000 kPa<br>m =5 g | 120.36 | Langmuir<br>($R^2$ > 099) | [39] |
| ERS-8 | T = 303 K<br>p = 0−1000 kPa<br>m = 5 g | 192.44 | Langmuir<br>($R^2$ > 099) | [39] |

| Adsorbents | Conditions | Capacity, mg/g | Langmuir/Freundlich | References |
|---|---|---|---|---|
| TH300 | [$H_2S$] = 50–400 ppm<br>m = 3 g<br>Q = 2.5 L/min | 30.96 | Langmuir<br>($R^2$ = 099) | [3] |
| 200-TP-Zn | T = 298 K<br>[$H_2S$] = 1000–3000 ppm<br>m = 10 g<br>Q = 1 L/min | 333.3 | Langmuir<br>($R^2$ = 0.9926) | This study |

*Regeneration adsorbent*

The reusability of 200-Zn/TP material was investigated with different desorption methods, including heating (200, 300, and 400 °C) and air blowing (2 L/min). The result in Fig. 14 indicates that the adsorption capacity was different when the material was desorbed under different conditions and was much lower than the first adsorption capacity. When using the calcination method, the higher the temperature of the material being desorbed, the lower the adsorption capacity or the lower the adsorption efficiency achieved at reuse. This may be because the high temperature (higher than the processing temperature) could break the original structure of the material, thus reducing the adsorption efficiency. When using the method of air blowing through the material column, the adsorption capacity of the reuse is higher than that of the regenerated materials by the calcination method, reaching 105.5 mg$H_2S$/g (reduced by 2.74 times compared to the original). In general, the results show that the efficiency of material reuse is not high. This may be because the mesopore structure of the starting material (Fig. 10) is not suitable for multiple reuse. In addition, the adsorption process of $S^{2-}$ on the surface of the adsorbent as waste sludge and the interaction between $S^{2-}$ and the adsorption centers can take place according to complicated processes, requiring further research to draw a suitable conclusion. Therefore, further study is needed to improve the regeneration of the adsorbent, in which, the partial oxidation of $H_2S$ to elemental sulfur ($S^0$) should be focused to recover $S^0$ as a valuable product. Otherwise, without an effective recovery method, the adsorbed material with saturated $H_2S$ must be disposed of as hazardous waste.

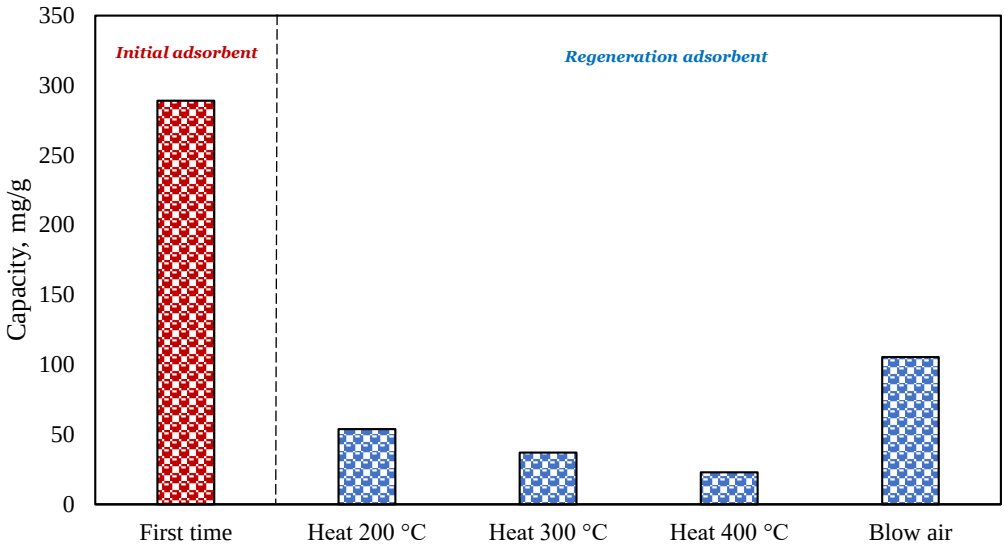


**Fig. 14. Adsorption capacity of regenerated adsorbent by heating (200, 300, 400 °C) and by blowing air (operating conditions: 2000 ppm of $H_2S$, 10 g of adsorbent, and flow rate of 1 L/min)**

## Conclusions

In the context of the global energy and resource crisis, utilizing one waste to treat another oneis a promising research direction that supports the circular economy. The research was successful in the modification of water treatment sludge into an effective adsorbent material. The experiments were conducted to assess the ability to adsorb $H_2S$ in order to introduce biogas filtration in practical applications. $H_2S$ adsorption capacity reaches 235.54 mg/g using Zn-modified sludge calcined at 200 °C under suitable conditions of inlet $H_2S$ concentration (1775 ± 169 ppm), adsorbent mass (5 g), and flow rate (1 L/min). The Langmuir maximum adsorption capacity was calculated to be 333.30 mg/g, which indicates that the material is promising for biogas filtrationHowever, the influence of environmental factors, particularly

the humidity of the input air, is an issue that needs clarification before the technology can be widely implemented. This study contributes an effective method for $H_2S$ removal using solid waste that provides both economic and environmental benefits for the biogas and water treatment industries.

## Acknowledgements

This research was funded by Vietnam National University Ho Chi Minh City (VNU-HCM) under grant no. C2022-20-27. The authors acknowledge the support of time and facilities from Ho Chi Minh City University of Technology (HCMUT), VNU-HCM, for this study.

## References

[1] Konkol, I., Cebula, J., Cenian, A. (2021). Oxidization of hydrogen sulfide in biogas by manganese (IV) oxide particles. *Environmental Engineering Research, 26*(2). doi: 10.4491/eer.2019.343.

[2] Triet, L. M., Thiep, N. N. (2013). Research and propose technology to treat and utilize sludge and water separated from sludge of water supply plants in Ho Chi Minh City (in Vietnamese). *Environment, 57*, 57–61.

[3] Lam Pham Thanh Hien, Le Nguyen Dang Khoa, Dang Van Thanh, Nguyen Thi Hieu, Tran Thi Phi Oanh, Vo Thi Thanh Thuy, Huy, N. N. (2021). Utilization of Alum Sludge from Water Treatment Plant as an Adsorbent for Hydrogen Sulfide Removal. *SNRU Journal of Science and Technology, 13*(3), 117–125.

[4] Polruang, S., Banjerdkij, P., Sirivittayapakorn, S. (2017). Use of drinking water sludge as adsorbent for $H_2S$ gas removal from biogas. *Environment Asia, 10*(1), 73–80. doi:10.14456/ea.2017.9

[5] Nguyen, M. D., Adhikari, S., Mallya, D. S., Thomas, M., Surapaneni, A., Moon, E. M., Milne, N. A. (2022). Reuse of aluminium-based water treatment sludge for phosphorus adsorption: Evaluating the factors affecting and correlation between adsorption and sludge properties. *Environmental Technology & Innovation, 27*: 102717. doi: 10.1016/j.eti.2022.102717.

[6] Ahmad, W., Sethupathi, S., Kanadasan, G., Lau, L. C., Kanthasamy, R. (2021). A review on the removal of hydrogen sulfide from biogas by adsorption using sorbents derived from waste. R*eviews in Chemical Engineering, 37*(3), 407–431. doi: 10.1515/revce-2018-0048.

[7] Ren, B., Lyczko, N., Zhao, Y., Nzihou, A. (2020). Alum sludge as an efficient sorbent for hydrogen sulfide removal: Experimental, mechanisms and modeling studies. *Chemosphere, 248*, 126010. https://doi.org/10.1016/j.chemosphere.2020.126010

[8] He, R., Zhang, X., Gu, J., Li, K., Guo, M., Jin, F., Jia, J., Sun, T. (2024). Iron-Based Catalysts Derived from Iron-Containing Sludge for Enhanced Catalytic Performance of H2S Selective Catalytic Oxidation. *ACS omega, 9*(27), 29691–29699. doi: 10.1021/acsomega.4c03115.

[9] Siswoyo, E., Qoniah, I., Lestari, P., Fajri, J. A., Sani, R. A., Sari, D. G., Boving, T. (2019). Development of a floating adsorbent for cadmium derived from modified drinking water treatment plant sludge. *Environmental Technology & Innovation,* 14, 100312. doi: 10.1016/j.eti.2019.01.006.

[10] Nguyen, T.D. (2018). The maximum absorption capacities of γ-FeOOH, α-FeOOH, γ-$Fe_2O_3$ and α-$Fe_2O_3$ nanoparticles for As(V) and As(III). *Science and Technology Development Journal - Natural Sciences, 1*(6), 237–246. doi: 10.32508/stdjns.v1i6.634.

[11] Sriram, G., Uthappa, U. T., Losic, D., Kigga, M., Jung, H.-Y., Kurkuri, M. D. (2020). Mg–Al-Layered Double Hydroxide (LDH) Modified Diatoms for Highly Efficient Removal of Congo Red from Aqueous Solution. *Applied Sciences, 10*(7), 2285. doi: 10.3390/app10072285

[12] Auerbach, S.M., Carrado, K.A., Dutta, P.K. (2004). *Handbook of layered materials*. CRC Press.

[13] Yuan, Y., Huang, L., Zhang, T.C., Ouyang, L., Yuan, S. (2021). One-step synthesis of $ZnFe_2O_4$-loaded biochar derived from leftover rice for high-performance H2S removal. *Separation and Purification Technology, 279,* 119686. doi: 10.1016/j.seppur.2021.119686.

[14] Othman, M.A., Zahid W.M., Abasaeed, A.E. (2013). Selectivity of layered double hydroxides and their derivative mixed metal oxides as sorbents of hydrogen sulfide. *J Hazard Mater, 254-255*, 221–227. doi: 10.1016/j.jhazmat.2013.03.030.

[15] Nguyen Nhat Huy, Vo Thi Thanh Thuy, Nguyen Hung Thang, Nguyen Thi Thuy, Le Thi Quynh, Tran Tien Khoi, Dang Van Thanh (2019). Facile one-step synthesis of zinc oxide nanoparticles by ultrasonic-assisted precipitation method and its application for $H_2S$ adsorption in air. *Journal of Physics and Chemistry of Solids, 132,* 99–103. doi: 10.1016/j.jpcs.2019.04.018.

[16] Zhang, Q., You, N., Wang, J., Xu, Y., Zhang, K., Wang, S. (2024). Combined Effect of Oxygen Vacancies and Mesopore Sizes in ZnO/$SiO_2$ Adsorbents on Boosting the H2S Removal Efficiency in Moist Conditions. *Advanced Functional Materials, 34*(49), 2409214. doi: 10.1002/adfm.202409214.

[17] Han, R., Zou, W., Zhang, Z., Shi, J., Yang, J. (2006). Removal of copper(II) and lead(II) from aqueous solution by manganese oxide coated sand I. Characterization and kinetic study. *J Hazard Mater, 137*(1), 384-395. doi: 10.1016/j.jhazmat.2006.02.021.

[18] Lǔ, J., Liu, H., Liu, R., Zhao, X., Sun, L., Qu, J. (2013). Adsorptive removal of phosphate by a nanostructured Fe–Al–Mn trimetal oxide adsorbent. *Powder Technology,* 233, 146–154. doi: 10.1016/j.powtec.2012.08.024.

[19] Thanh Son Cam, Bui Quang Huy, Nguyen Thi Thuy, Lam Pham Thanh Hien, Juying Lei, Nguyen Nhat Huy. (2024). Development of low-cost adsorbents derived from sludge of groundwater treatment for gaseous hydrogen sulfide removal. *Energy Sources, Part A: Recovery, Utilization, and Environmental Effects, 46*(1), 3707–3719. doi: 10.1080/15567036.2024.2322017.

[20] Zeng, H., Sun, S., Xu, K., Zhao, W., Hao, R., Zhang, J., Li, D. (2022). Adsorption of As (V) by magnetic alginate-chitosan porous beads based on iron sludge. *Journal of Cleaner Production, 359,* 132117. doi: 10.1016/j.jclepro.2022.132117.

[21] Zhuang, J., Li, M., Pu, Y., Ragauskas, A., Yoo, C. (2020). Observation of Potential Contaminants in Processed Biomass Using Fourier Transform Infrared Spectroscopy. *Applied Sciences, 10*(12), 4345. doi: 10.3390/app10124345.

[22] Galván-Ruiz, M., Hernández, J., Baños, L., Noriega-Montes, J., Rodríguez-García, M. E. (2009). Characterization of Calcium Carbonate, Calcium Oxide, and Calcium Hydroxide as Starting Point to the Improvement of Lime for Their Use in Construction.

*Journal of Materials in Civil Engineering,* 21(11), 694-698. doi: 10.1061/(asce)0899-1561(2009)21:11(694).

[23] Kan, C.-C., Ibe, A. H., Rivera, K. K. P., Arazo, R. O., de Luna, M. D. G. (2017). Hexavalent chromium removal from aqueous solution by adsorbents synthesized from groundwater treatment residuals. *Sustainable Environment Research, 27*(4), 163–171. doi: 10.1016/j.serj.2017.04.001.

[24] Kiefer, J., Stärk, A., Kiefer, A., Glade, H. (2018). Infrared Spectroscopic Analysis of the Inorganic Deposits from Water in Domestic and Technical Heat Exchangers. *Energies, 11*(4), 798. doi: 10.3390/en11040798.

[25] Prasad, P. S. R. (2005). Direct formation of the -$CaSO_4$ phase in dehydration process of gypsum: In situ FTIR study. *American Mineralogist, 90*(4), 672–678. doi: 10.2138/am.2005.1742.

[26] Bu, H., Ju, Y., Tan, J., Wang, G., Li, X. (2015). Fractal characteristics of pores in non-marine shales from the Huainan coalfield, eastern China. *Journal of Natural Gas Science and Engineering, 24*, 166–177. doi: 10.1016/j.jngse.2015.03.021.

[27] Lam Pham Thanh Hien, Thanh Son Cam, Pham Hong Phuc, Nguyen Thi Thuy, Vo Thi Thanh Thuy, Dang Van Thanh, Nguyen Nhat Huy (2024). Adsorption and partial catalytic oxidation of hydrogen sulfide to elemental sulfur using facilely prepared materials derived from sludge of groundwater treatment. *Environmental Progress & Sustainable Energy,* e14383. doi: 10.1002/ep.14383.

[28] Belmabkhout, Y., De Weireld, G., Sayari, A. (2009). Amine-bearing mesoporous silica for $CO_2$ and $H_2S$ removal from natural gas and biogas. *Langmuir, 25*(23), 13275–13278. doi: 10.1021/la903238y.

[29] Bandosz, T. J. (2002). On the adsorption/oxidation of hydrogen sulfide on activated carbons at ambient temperatures. *Journal of Colloid and Interface Science, 246*(1), 1–20. doi: 10.1006/jcis.2001.7952.

[30] Daneshyar, A., Ghaedi, M., Sabzehmeidani, M. M., Daneshyar, A. (2017). $H_2S$ adsorption onto Cu-Zn-Ni nanoparticles loaded activated carbon and Ni-Co nanoparticles loaded gamma-$Al_2O_3$: Optimization and adsorption isotherms. *J Colloid Interface Sci, 490*, 553–561. doi: 10.1016/j.jcis.2016.11.068.

[31] Choo, H. S., Lau, L. C., Mohamed, A. R., Lee, K. T., Technology. (2013). Hydrogen sulfide adsorption by alkaline impregnated coconut shell activated carbon. *Journal of Engineering Science, 8*(6), 741–753.

[32] Lam Pham Thanh Hien, Le Truong Anh Huy, Pham Dan Thanh, Le Nguyen Dang Khoa, Bui Khanh Le, Le Thi Kieu Thi, Vo Thi Thanh Thuy, Huy, N. N. (2019). Preparation of activated red mud and its application for removal of hydrogen sulfide in air. *Science & Technology Development Journal-Engineering and Technology, 2*(SI2), SI40–SI45. doi: 10.32508/stdjet.v3i2.474.

[33] Wang, Q. (2023). Optimization of Oil-Sludge-Based Adsorbents for the Treatment of Toxic H2S in Oilfield Gases: Preparation, Modification, Characterization, and Adsorption Mechanism. *Energy & Fuels, 37*(22), 17399–17410. DOI: 10.1021/acs.energyfuels.3c03347.

[34] McCabe, W. L., Smith, J. C., Harriott, P. (2005). *Unit Operations of Chemical Engineering* (7th ed.). Boston: McGraw-Hill Education.

[35] Wang, S., Nam, H., Nam, H. (2020). Preparation of activated carbon from peanut shell with KOH activation and its application for $H_2S$ adsorption in confined space. *Journal of Environmental Chemical Engineering, 8*(2), 103683. doi: 10.1016/j.jece.2020.103683.

[36] Sun, Y., Zhang, J. P., Wen, C., Zhang, L. (2016). An enhanced approach for biochar preparation using fluidized bed and its application for $H_2S$ removal. *Chemical Engineering and Processing: Process Intensification, 104*, 1–12. doi: 10.1016/j.cep.2016.02.006.

[37] Maghsoudi, H., Soltanieh, M., Bozorgzadeh, H., Mohamadalizadeh, A. (2013). Adsorption isotherms and ideal selectivities of hydrogen sulfide and carbon dioxide over methane for the Si-CHA zeolite: comparison of carbon dioxide and methane adsorption with the all-silica DD3R zeolite. *Adsorption, 19*(5), 1045–1053. doi: 10.1007/s10450-013-9528-1.

[38] Tagliabue, M., Bellussi, G., Broccia, P., Carati, A., Millini, R., Pollesel, P., Rizzo, C. (2012). High pressure hydrogen sulphide adsorption on silica–aluminas. *Chemical Engineering Journal, 210*, 398–403. doi: 10.1016/j.cej.2012.08.076.